

# Observation of the Decay $K_L \rightarrow \mu^+ \mu^- \gamma \gamma$ .

A. Alavi-Harati<sup>12</sup>, I.F. Albuquerque<sup>10</sup>, T. Alexopoulos<sup>12</sup>, M. Arenton<sup>11</sup>, K. Arisaka<sup>2</sup>, S. Averitte<sup>10</sup>, A.R. Barker<sup>5</sup>, L. Bellantoni<sup>7</sup>, A. Bellavance<sup>9</sup>, J. Belz<sup>10</sup>, R. Ben-David<sup>7</sup>, D.R. Bergman<sup>10</sup>, E. Blucher<sup>4</sup>, G.J. Bock<sup>7</sup>, C. Bown<sup>4</sup>, S. Bright<sup>4</sup>, E. Cheu<sup>1</sup>, S. Childress<sup>7</sup>, R. Coleman<sup>7</sup>, M.D. Corcoran<sup>9</sup>, G. Corti<sup>11</sup>, B. Cox<sup>11</sup>, M.B. Crisler<sup>7</sup>, A.R. Erwin<sup>12</sup>, R. Ford<sup>7</sup>, A. Glazov<sup>4</sup>, A. Golossanov<sup>11</sup>, G. Graham<sup>4</sup>, J. Graham<sup>4</sup>, K. Hagan<sup>11</sup>, E. Halkiadakis<sup>10</sup>, K. Hanagaki<sup>8</sup>, M. Hazumi<sup>8</sup>, S. Hidaka<sup>8</sup>, Y.B. Hsiung<sup>7</sup>, V. Jejer<sup>11</sup>, J. Jennings<sup>2</sup>, D.A. Jensen<sup>7</sup>, R. Kessler<sup>4</sup>, H.G.E. Kobrak<sup>3</sup>, J. LaDue<sup>5</sup>, A. Lath<sup>10†</sup>, A. Ledovskoy<sup>11</sup>, P.L. McBride<sup>7</sup>, A.P. McManus<sup>11</sup>, P. Mikelsons<sup>5</sup>, E. Monnier<sup>4,\*</sup>, T. Nakaya<sup>7</sup>, K.S. Nelson<sup>11</sup>, H. Nguyen<sup>7</sup>, V. O'Dell<sup>7</sup>, M. Pang<sup>7</sup>, R. Pordes<sup>7</sup>, V. Prasad<sup>4</sup>, C. Qiao<sup>4</sup>, B. Quinn<sup>4</sup>, E.J. Ramberg<sup>7</sup>, R.E. Ray<sup>7</sup>, A. Roodman<sup>4</sup>, M. Sadamoto<sup>8</sup>, S. Schnetzer<sup>10</sup>, K. Senyo<sup>8</sup>, P. Shanahan<sup>7</sup>, P.S. Shawhan<sup>4</sup>, W. Slater<sup>2</sup>, N. Solomey<sup>4</sup>, S.V. Somalwar<sup>10</sup>, R.L. Stone<sup>10</sup>, I. Suzuki<sup>8</sup>, E.C. Swallow<sup>4,6</sup>, R.A. Swanson<sup>3</sup>, S.A. Taegar<sup>1</sup>, R.J. Tesarek<sup>10</sup>, G.B. Thomson<sup>10</sup>, P.A. Toale<sup>5</sup>, A. Tripathi<sup>2</sup>, R. Tschirhart<sup>7</sup>, Y.W. Wah<sup>4</sup>, J. Wang<sup>1</sup>, H.B. White<sup>7</sup>, J. Whitmore<sup>7</sup>, B. Winstein<sup>4</sup>, R. Winston<sup>4</sup>, T. Yamanaka<sup>8</sup>, E.D. Zimmerman<sup>4</sup>

<sup>1</sup> University of Arizona, Tucson, Arizona 85721

<sup>2</sup> University of California at Los Angeles, Los Angeles, California 90095

<sup>3</sup> University of California at San Diego, La Jolla, California 92093

<sup>4</sup> The Enrico Fermi Institute, The University of Chicago, Chicago, Illinois 60637

<sup>5</sup> University of Colorado, Boulder, Colorado 80309

<sup>6</sup> Elmhurst College, Elmhurst, Illinois 60126

<sup>7</sup> Fermi National Accelerator Laboratory, Batavia, Illinois 60510

<sup>8</sup> Osaka University, Toyonaka, Osaka 560 Japan

<sup>9</sup> Rice University, Houston, Texas 77005

<sup>10</sup> Rutgers University, Piscataway, New Jersey 08855

<sup>11</sup> The Department of Physics and Institute of Nuclear and Particle Physics, University of Virginia, Charlottesville, Virginia 22901

<sup>12</sup> University of Wisconsin, Madison, Wisconsin 53706

\* On leave from C.P.P. Marseille/C.N.R.S., France

† To whom correspondence should be addressed.

We have observed the decay  $K_L \rightarrow \mu^+ \mu^- \gamma \gamma$  at the KTeV experiment at Fermilab. This decay presents a formidable background to the search for new physics in  $K_L \rightarrow \pi^0 \mu^+ \mu^-$ . The 1997 data yielded a sample of 4 signal events, with an expected background of  $0.155 \pm 0.081$  events. The branching ratio is  $\mathcal{B}(K_L \rightarrow \mu^+ \mu^- \gamma \gamma) = (10.4^{+7.5}_{-5.9} \text{ (stat)} \pm 0.7 \text{ (sys)}) \times 10^{-9}$  with  $m_{\gamma\gamma} \geq 1 \text{ MeV}/c^2$ , consistent with a QED calculation which predicts  $(9.1 \pm 0.8) \times 10^{-9}$ .

In this paper we present the first measurement of the branching ratio for  $K_L \rightarrow \mu^+ \mu^- \gamma \gamma$ . This decay is expected to proceed mainly via the Dalitz decay  $K_L \rightarrow \mu^+ \mu^- \gamma$  with an internal bremsstrahlung photon. This decay is one of a family of radiative decays ( $K_L \rightarrow \mu^+ \mu^- \gamma$ ,  $K_L \rightarrow \mu^+ \mu^- \gamma \gamma$ ,  $K_L \rightarrow e^+ e^- \gamma$ ,  $K_L \rightarrow e^+ e^- \gamma \gamma$ ) which are under study at KTeV and elsewhere [1,2]. The decay  $K_L \rightarrow \mu^+ \mu^- \gamma \gamma$  presents a formidable background to the search for direct CP violation and new physics in  $K_L \rightarrow \pi^0 \mu^+ \mu^-$  decays [3].

The measurement presented here was performed as part of the KTeV experiment, which has been described elsewhere [4]. The experiment used two nearly parallel  $K_L$  beams created by 800 GeV protons incident on a BeO target. The decays used in our studies were collected in a region approximately 65 meters long, situated 94 meters from the production target. The fiducial volume was surrounded by a photon veto system used to reject events in which photons missed the calorimeter. The charged particles were detected by four drift chambers, each consisting of one horizontal and one vertical pair of planes, with typical resolution of 70  $\mu\text{m}$  per plane pair. Two drift chambers were situated on either side of an analysis magnet which imparted 205 MeV/c of transverse momentum to charged particles. The drift chambers were followed by a trigger hodoscope bank, and a 3100 element pure CsI calorimeter with electromagnetic energy resolution of  $\sigma(E)/E = 0.45\% \oplus 2.0\%/\sqrt{E(\text{GeV})}$ . The calorimeter was followed by a muon filter composed of a 10 cm thick lead wall and three steel walls totalling 511 cm. Two planes of scintillators situated after the third steel wall served to identify muons. The planes had 15 cm segmentation, one horizontal, the other vertical.

The trigger for the signal events required hits in the upstream drift chambers consistent with two tracks, as well as two hits in the trigger hodoscopes. The calorimeter was required to have at least one cluster with over 1 GeV in energy, within a narrow (20 ns) time gate. The muon counters were required to have at least two hits. In addition, preliminary online identification of these decays required reconstruction of two track candidates originating from a loosely-defined vertex, and each of those track candidates was required to point to a cluster in the calorimeter with energy less than

5 GeV. A separate trigger was used to collect  $K_L \rightarrow \pi^+\pi^-\pi^0$  decays which were used for normalization. This trigger was similar to the signal trigger but had no requirements on hits in the muon hodoscopes or clusters in the calorimeter. The preliminary online identification was performed on the normalization sample as well, but no energy requirements were made on clusters pointed to by the tracks. The normalization mode trigger was prescaled by a factor of 500:1.

The main background to  $K_L \rightarrow \mu^+\mu^-\gamma\gamma$  was the Dalitz decay  $K_L \rightarrow \mu^+\mu^-\gamma$  with an additional cluster in the calorimeter coincident with but not due to the decay. Such an “accidental” cluster could appear as a photon. Additional backgrounds were  $K_L \rightarrow \pi^+\pi^-\pi^0$  decays with the charged pions misidentified as muons due to pion decay or pion punchthrough the filter steel, and  $K_L \rightarrow \pi^\pm\mu^\mp\nu$  decays ( $K_{\mu 3}$ ) with both charged pion misidentification and accidental cluster contributions. Other contributions, such as  $K_L \rightarrow \pi^+\pi^-$  decays and  $K_L \rightarrow \pi^+\pi^-\gamma$  decays, were negligible.

Offline analysis of the signal required the full reconstruction of exactly two tracks. The vertex reconstructed from the two tracks was required to fall between 100 meters and 158 meters from the target. In order to reduce backgrounds due to pion decay in flight, we required that the track segments upstream and downstream of the analysis magnet matched to within 1 mm at the magnet bend plane. Further, we required the  $\chi^2$  calculated from the reconstructed two-track vertex be less than 10 for 1 degree of freedom. Tracks were required to have momenta equal to or greater than 10 GeV/c to put them above threshold for passing through the filter steel but below 100 GeV/c to ensure well measured track momenta. Since muons typically deposit  $\sim 400$  MeV in the calorimeter, we required the energy deposited by each track be 1 GeV or less. In addition, we required two non-adjacent hits in both the vertically and horizontally segmented muon counters.

Figure 1 shows the expected distribution of cluster energy due to photons from  $K_L \rightarrow \mu^+\mu^-\gamma$  events and those from accidental sources. Accidental clusters in the calorimeter were typically of low energy. Events were required to have two calorimeter clusters consistent with photons with no tracks pointing to them. One of these clusters was required to have greater than 10 GeV of energy, thus reducing backgrounds due to accidental clusters.

In order to reject backgrounds from decays that contained a  $\pi^0$ , the invariant mass of the two photons,  $m_{\gamma\gamma}$ , was required to be less than  $130 \text{ MeV}/c^2$ . Approximately 8% of the  $K_L \rightarrow \pi^+\pi^-\pi^0$  decays in which the charged pions decay to muons survived the  $m_{\gamma\gamma}$  cut because the mismeasurement of the charged vertex smeared the  $m_{\gamma\gamma}$  distribution. In order to remove these events, we constructed a variable ( $R_{\parallel}^{\pi\pi}$ ) defined as

$$R_{\parallel}^{\pi\pi} = \frac{(m_K^2 - m_{\pi\pi}^2 - m_{\pi^0}^2)^2 - 4m_{\pi\pi}^2 m_{\pi^0}^2 - 4m_K^2 p_{\perp\pi\pi}^2}{p_{\perp\pi\pi}^2 + m_{\pi\pi}^2} \quad (1)$$

where  $m_K$  is the kaon mass,  $m_{\pi\pi}$  is the invariant mass of the two tracks assuming they are due to charged pions,  $p_{\perp\pi\pi}^2$  is the square of the transverse momentum of the two pions with respect to a line connecting the target to the two-track vertex, and  $m_{\pi^0}$  is the mass of the  $\pi^0$ . This quantity is proportional to the square of the longitudinal momentum of the  $\pi^0$  in a frame along the  $K_L$  flight direction where the  $\pi^+\pi^-$  pair has no longitudinal momentum.

Figure 2 shows the expected distribution of  $R_{\parallel}^{\pi\pi}$  for the signal (using an  $\mathcal{O}(\alpha)$  QED matrix element), and the  $K_L \rightarrow \pi^+\pi^-\pi^0$  background. By requiring  $R_{\parallel}^{\pi\pi}$  to be -0.06 or less, 92.7% of the remaining  $K_L \rightarrow \pi^+\pi^-\pi^0$  background was eliminated.

The invariant mass of the two tracks assuming muons,  $m_{\mu\mu}$ , provided a way to reduce backgrounds due to  $K_{\mu 3}$  decays. Figure 3 shows the expected distribution of  $m_{\mu\mu}$  for the signal and background. We required  $m_{\mu\mu}$  to be less than  $340 \text{ MeV}/c^2$ . This cut eliminated 92.9% of the  $K_{\mu 3}$  events.

The cosine of the angle between the two photons in the kaon rest frame,  $\cos\theta_{\gamma\gamma}$ , was also used to reject  $K_{\mu 3}$  decays. The distribution of  $\cos\theta_{\gamma\gamma}$  for the signal peaks at -1 corresponding to anti-collinear emission of the two photons. The  $K_{\mu 3}$  background, which has two accidental clusters identified as photons, displays no such correlation. Figure 4 shows the expected  $\cos\theta_{\gamma\gamma}$  distribution for signal and  $K_{\mu 3}$  background. We required  $\cos\theta_{\gamma\gamma}$  to be -0.3 or less. This cut rejected 85.3% of the remaining  $K_{\mu 3}$  events.

We also required the transverse shower shape for the photon clusters to be consistent with that expected from an electromagnetic process. The  $\chi^2$  of the spatial distribution of energy deposited in the calorimeter was used to identify clusters as photons. This cut reduced the remaining backgrounds due to accidental energy by a factor of 4.5 while retaining 98.8% of the signal events.

In order to estimate the amount of background in the signal region, we simulated all the leading sources of background. Our simulation incorporated both charged pion decay in flight and punch-through the filter steel. The punch-through rate was a function of  $\pi^\pm$  momentum, determined by a  $K_L \rightarrow \pi e \nu$  control sample. The effect of accidental activity was simulated by overlaying Monte Carlo events with data from a random trigger that had a rate proportional to the beam intensity. The estimated background level is detailed in Table I. A total of  $0.155 \pm 0.081$  background events are expected within the signal region. This region is defined by the invariant mass of the  $\mu^+\mu^-\gamma\gamma$

( $m$ ), and square of the transverse momentum of the four particles with respect to a line connecting the target to the decay vertex ( $P_{\perp}^2$ ) of the four particles in the final state:  $492 \text{ MeV}/c^2 < m < 504 \text{ MeV}/c^2$ , and  $P_{\perp}^2 \leq 100 (\text{MeV}/c)^2$ . After all the cuts we observed four events in the signal region. Figure 5 shows the  $m$  vs. the  $P_{\perp}^2$  for events with all but these cuts. A linear extrapolation of the high  $P_{\perp}^2$  data in this figure yields a background estimate of  $0.25 \pm 0.10$  events, consistent with the expectation from Monte Carlo studies. To further test the background estimate with higher statistics we removed the cluster shape  $\chi^2$  cut and verified that the data matched the prediction in  $m$  and  $P_{\perp}^2$  side bands. The probability of observing four events in the signal region due to fluctuation of the background is  $2.1 \times 10^{-5}$ , corresponding to a  $4.2 \sigma$  fluctuation of the estimated background. The branching ratio for  $K_L \rightarrow \mu^+ \mu^- \gamma \gamma$  was calculated by normalizing the four signal events to a sample of  $K_L \rightarrow \pi^+ \pi^- \pi^0$  events, collected with the prescaled normalization trigger. For the normalization events  $m_{\gamma\gamma}$  was required to be within  $3 \text{ MeV}/c^2$  of  $m_{\pi^0}$ , and the  $R_{\parallel}^{\pi\pi}$  and muon counter hit requirements were not enforced. The acceptance of these events was calculated to be  $8.1\%$  via Monte Carlo. We determined that  $(2.68 \pm 0.04) \times 10^{11}$   $K_L$  within an energy range of 20 to 220 GeV decayed between 90 and 160 meters from the target. The acceptance of the signal was  $(0.14 \pm 0.01)\%$ , so  $\mathcal{B}(K_L \rightarrow \mu^+ \mu^- \gamma \gamma) = (10.4_{-5.9}^{+7.5} (\text{stat})) \times 10^{-9}$  with  $m_{\gamma\gamma} \geq 1 \text{ MeV}/c^2$  which was the cutoff we used in generating the Monte Carlo events.

We have calculated the branching ratio for this  $K_L$  Dalitz decay by performing a numerical integration of the tree-level ( $\mathcal{O}(\alpha)$ )  $K_L \rightarrow \mu\mu\gamma\gamma$  matrix element with an  $m_{\gamma\gamma} \geq 1 \text{ MeV}/c^2$  cutoff. We performed a similar integration of the  $K_L \rightarrow \mu\mu\gamma$  matrix element, which included contributions due to virtual photon loops and emission of soft bremsstrahlung photons. Both integrations assumed unit form factors. The ratio of partial widths is  $2.789\%$ . Multiplying this ratio with the measured value for  $\mathcal{B}(K_L \rightarrow \mu\mu\gamma) = (3.26 \pm 0.28) \times 10^{-7}$  [2] yields  $\mathcal{B}(K_L \rightarrow \mu\mu\gamma\gamma) = (9.1 \pm 0.8) \times 10^{-9}$ .

The four-body phase space for  $K_L \rightarrow \mu^+ \mu^- \gamma \gamma$  can be parametrized by five variables, as in reference [5].

Figure 6 shows the distribution of the energy asymmetry of the photon pair ( $y_{\gamma}$ ), the angle between the normals to the planes containing the  $\mu^+ \mu^-$  and  $\gamma\gamma$  in the center of mass ( $\phi$ ), and the minimum angle from any muon to any photon ( $\Theta_{\text{MIN}}$ ). The distribution of these kinematic variables for the four signal events is consistent with expectations.

We examined several possible sources of systematic uncertainty in the measurement. The largest effects were due to a possible miscalibration of the calorimeter resulting in a mismeasurement of the photon energies, and particle identification. If we conservatively assume a  $0.7\%$  miscalibration of the calorimeter we obtain a  $5.11\%$  systematic error. The uncertainty due to muon identification was determined to be  $4.2\%$  by comparing the  $K_L$  flux with that obtained by using  $K_{\mu 3}$  decays. The uncertainty in the  $K_L \rightarrow \pi^+ \pi^- \pi^0$  branching ratio is  $1.59\%$ . Adding these and other smaller contributions detailed in Table II in quadrature we assigned a total systematic uncertainty of  $6.95\%$  to the branching ratio measurement.

In summary we have determined the branching ratio to be  $\mathcal{B}(K_L \rightarrow \mu^+ \mu^- \gamma \gamma) = (10.4_{-5.9}^{+7.5} (\text{stat}) \pm 0.7 (\text{sys})) \times 10^{-9}$  with  $m_{\gamma\gamma} \geq 1 \text{ MeV}/c^2$ . Defining the acceptance with a  $10 \text{ MeV}$  infrared cutoff for photon energies in the kaon frame ( $E_{\gamma}^*$ ), our result is  $\mathcal{B}(K_L \rightarrow \mu^+ \mu^- \gamma \gamma; E_{\gamma}^* \geq 10 \text{ MeV}) = (1.42_{-0.8}^{+1.0} (\text{stat}) \pm 0.10 (\text{sys})) \times 10^{-9}$ . This is the first observation of this decay and is consistent with theoretical predictions.

We gratefully acknowledge the support and effort of the Fermilab staff and the technical staffs of the participating institutions for their vital contributions. This work was supported in part by the U.S. DOE, The National Science Foundation and The Ministry of Education and Science of Japan. In addition, A.R.B., E.B. and S.V.S. acknowledge support from the NYI program of the NSF; A.R.B. and E.B. from the Alfred P. Sloan Foundation; E.B. from the OJI program of the DOE; K.H., T.N., K.S., and M.S. from the Japan Society for the Promotion of Science.

- [1] Barr *et al.* Phys. Lett. **B240**, 283 (1990);  
Ohl *et al.* Phys. Rev. Lett. **65**, 1407 (1990);  
T. Nakaya *et al.* Phys. Rev. Lett. **73**, 2169 (1994);  
Morse *et al.* Phys. Rev. **D45**, 36 (1992).
- [2] V. Fanti *et al.* Z. Phys. **C76**, 653 (1997);  
M. Spencer *et al.* Phys. Rev. Lett. **74**, 3323 (1995).
- [3] A. Alavi-Harati *et al.* "Search for the Decay  $K_L \rightarrow \pi^0 \mu^+ \mu^-$ ", Submitted to Phys. Rev. Lett.
- [4] K. Hanagaki, Ph.D. Thesis, University of Osaka, Japan (August, 1998)  
**hep-ex/9907014**.

A. Alavi-Harati *et al.* Phys. Rev. Lett. **83**, 922 (1999).

C. Bown *et al.* Nuclear Instruments and Methods, **A369**, 248 (1996).

[5] H.B. Greenlee., Phys. Rev. **D42**, 3724 (1990).

TABLE I. The various backgrounds to  $K_L \rightarrow \mu^+ \mu^- \gamma \gamma$ .  $\pi^\pm$  can be mistaken for  $\mu^\pm$  due to decay (D) or punch-through (P). Accidental clusters in the calorimeter identified as photons are designated  $\gamma_{acc}$ .

Decay	Cause of $\mu$ misid	Events expected
$K_L \rightarrow \mu^+ \mu^- \gamma \gamma_{acc}$		$0.093 \pm 0.036$
$K_L \rightarrow \pi^+ \pi^- \pi^0$	DD	$< 0.056$
$K_L \rightarrow \pi^+ \pi^- \pi^0$	DP	$< 0.011$
$K_L \rightarrow \pi^+ \pi^- \pi^0$	PP	$< 0.011$
$K_L \rightarrow \pi^\pm \mu^\mp \nu + 2\gamma_{acc}$	D	$0.030 \pm 0.030$
$K_L \rightarrow \pi^\pm \mu^\mp \nu + 2\gamma_{acc}$	P	$0.032 \pm 0.032$
$K_L \rightarrow \pi^\pm \pi^0 \mu^\mp \nu$	D	$< 0.005$
$K_L \rightarrow \pi^\pm \pi^0 \mu^\mp \nu$	P	$< 0.004$
<b>Total</b>		$0.155 \pm 0.081$

TABLE II. Systematic and statistical sources of uncertainty. Sources marked with (\*) contribute to uncertainty in both the  $K_L$  flux and the acceptance for  $K_L \rightarrow \mu \mu \gamma \gamma$  relative to the acceptance for  $K_L \rightarrow \pi^+ \pi^- \pi^0$ ; other sources contribute only to the acceptance ratio.

Source	Relative Uncertainty
$BK_L \rightarrow \pi^+ \pi^- \pi^0$	1.59% (*)
Data statistics for $K_L \rightarrow \pi^+ \pi^- \pi^0$	0.16% (*)
Simulation statistics	0.22% (*)
Calorimeter scale and resolution	5.11%
Spectrometer scale and resolution	0.98%
Muon identification	4.20%
Signal trigger requirements	0.80%
Vertex quality requirement	0.24%
Spectrometer wire inefficiency	0.37%
Total	6.95%

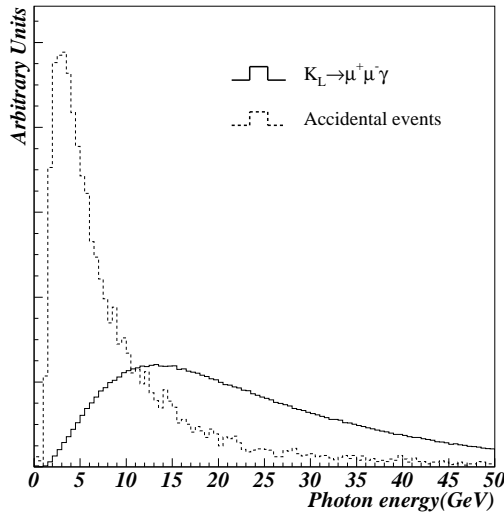


FIG. 1. Energy deposited in the calorimeter by photons from Monte Carlo simulations of  $K_L \rightarrow \mu^+ \mu^- \gamma$  events (solid) vs. accidental clusters (dashed) from data taken with a random trigger.

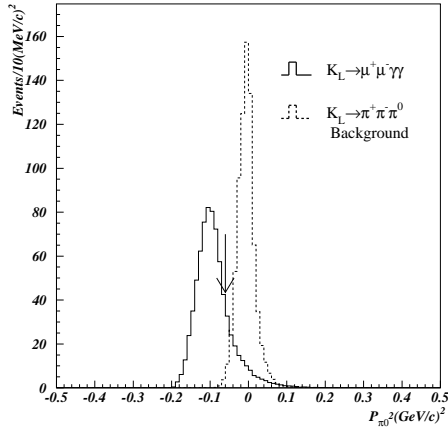


FIG. 2. The distribution of  $R_{\parallel}^{\pi\pi}$  (see text) from Monte Carlo simulations of the signal (solid) and backgrounds from  $K_L \rightarrow \pi^+\pi^-\pi^0$  (dashed) that remain after the  $m_{\gamma\gamma} < 130\text{MeV}/c^2$  requirement. The arrow indicates the cut at  $-0.06$ , above which events were discarded.

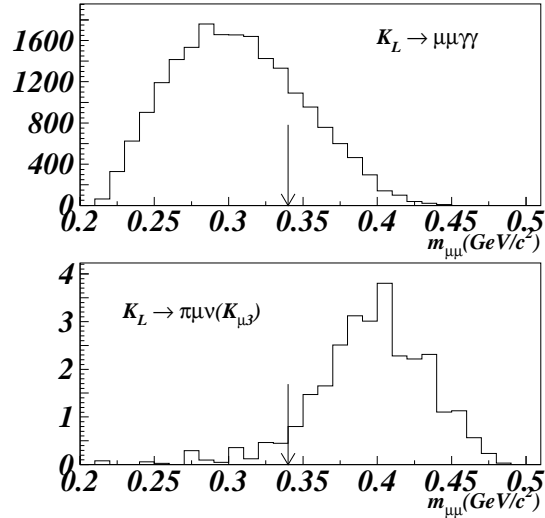


FIG. 3. The distribution of  $m_{\mu\mu}$  from Monte Carlo simulations of the signal (top) and backgrounds from  $K_{\mu 3}$  (bottom). The arrows indicate the cut at  $340\text{ MeV}/c^2$ , above which events were discarded.

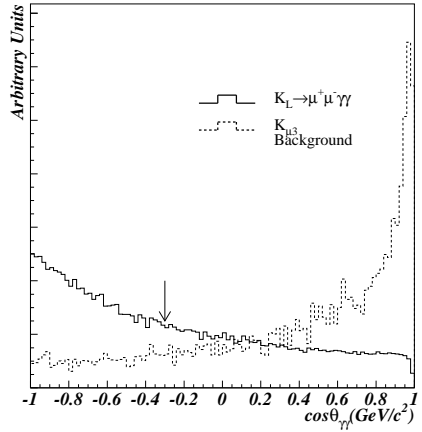


FIG. 4. The cosine of the angle between the two photons, from Monte Carlo simulations of the signal (solid) and  $K_{\mu 3}$  (dashed). The requirement of  $\leq 0.3$  is indicated by the arrow.

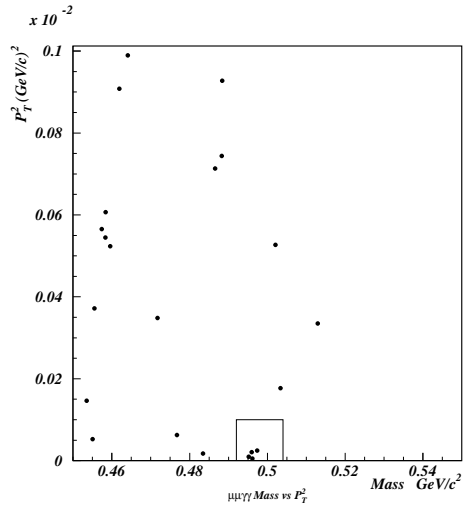


FIG. 5.  $m$  vs.  $P_{\perp}^2$  for the events that passed all other cuts. The box is drawn around the signal region, which contains 4 events.

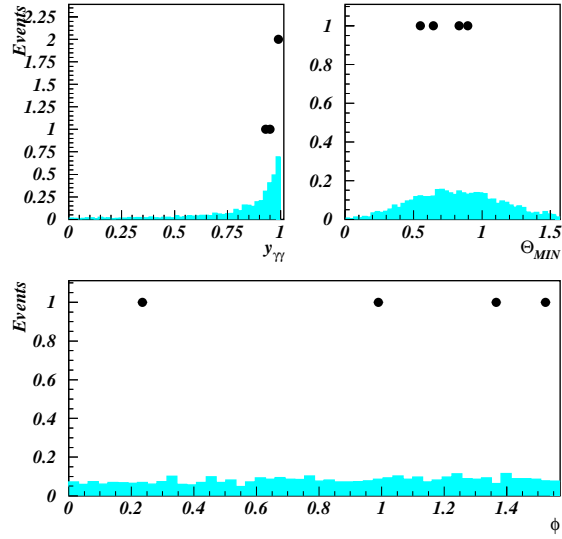


FIG. 6. The distributions for data (dots) and signal Monte Carlo (shaded) for the variables  $y_\gamma$ ,  $\Theta_{MIN}$ , and  $\phi$  as defined in the text.